

14773

Copy 208
RM L54H19

NACA RM L54H19

0143556

TECH LIBRARY KAFB, NM

NACA

RESEARCH MEMORANDUM

AN INVESTIGATION OF A SUPERSONIC AIRCRAFT CONFIGURATION
HAVING A TAPERED WING WITH CIRCULAR-ARC SECTIONS
AND 40° SWEEPBACK

AERODYNAMIC CHARACTERISTICS OF THE CONFIGURATION EQUIPPED
WITH A CANARD CONTROL SURFACE AT A MACH NUMBER OF 1.89

By M. Leroy Spearman and Edward B. Palazzo

Langley Aeronautical Laboratory
Langley Field, Va.

**NATIONAL ADVISORY COMMITTEE
FOR AERONAUTICS**

WASHINGTON

October 18, 1954

Classification cancelled (or changed to Unclassified)

By Authority of Navy Personnel Management Act
(OFFICER AUTHORIZED TO CHANGE)

By John F. Smith

John F. Smith
GRADE OF OFFICER MAKING CHANGE)

29 May 61
DATE



NATIONAL ADVISORY COMMITTEE FOR AERONAUTICS

RESEARCH MEMORANDUM

AN INVESTIGATION OF A SUPERSONIC AIRCRAFT CONFIGURATION
HAVING A TAPERED WING WITH CIRCULAR-ARC SECTIONS
AND 40° SWEEPBACK

AERODYNAMIC CHARACTERISTICS OF THE CONFIGURATION EQUIPPED
WITH A CANARD CONTROL SURFACE AT A MACH NUMBER OF 1.89

By M. Leroy Spearman and Edward B. Palazzo

SUMMARY

An investigation has been conducted in the Langley 4- by 4-foot supersonic pressure tunnel to determine the aerodynamic characteristics of a supersonic aircraft configuration equipped with a canard control surface (in addition to a rearward horizontal stabilizer) at a Mach number of 1.89. The model had a 40° sweptback tapered wing with an aspect ratio of 4 and 10-percent-thick circular-arc sections normal to the quarter-chord line. The canard surface had a total area about one-twelfth of the total wing area and was located 2.27 mean aerodynamic chord lengths ahead of the reference center of gravity.

The results indicated that the maximum trim lift coefficient might be increased from about 0.26 for the model without the canard to about 0.84 for the model with the canard. The ratio of lift to drag at the maximum lift coefficient was slightly less than 2. The neutral-point location varied from about 36 percent of the mean aerodynamic chord for a zero canard deflection to about 64 percent for a canard deflection of 30°. The presence of the canard at zero deflection and zero angle of attack had little effect on the characteristics in sideslip.

INTRODUCTION

Among the problems that may be encountered during flight at extremely high altitudes is that of maintaining satisfactory stability and control. High angles of attack would be required for trimmed level flight at high

altitudes and in addition the ability to reach high angles of attack might be required for the purpose of decelerating.

In general, it has been found difficult to attain high angles of attack at supersonic speeds with current airplane designs largely because of the increased longitudinal stability that occurs in going from subsonic to supersonic flight and partly because of decreased control effectiveness. (See reference 1 for example.)

A possible means of increasing the maximum angle-of-attack capabilities for conventional tail-rearward designs would be through the use of a canard control surface installed for the dual purpose of reducing the longitudinal stability and providing additional longitudinal control. Such a device, of course, would also reduce the stability at subsonic speeds and at these speeds it would probably be necessary to allow the canard surface to float freely.

The present tests were conducted to determine the effectiveness of a canard-type surface in reducing the static longitudinal stability and increasing the trim-angle-of-attack capabilities of a model of a supersonic aircraft configuration at a Mach number of 1.89. In order to simulate high altitudes the tests were made at a tunnel stagnation pressure of 2 pounds per square inch absolute corresponding to a Reynolds number of 0.28×10^6 (based on the wing mean aerodynamic chord) and to a pressure altitude of about 88,000 feet.

COEFFICIENTS AND SYMBOLS

In the presentation of the experimental results, the force and moment coefficients are referred to the stability axis system (fig. 1) with the reference-center-of-gravity location at the 25-percent point of the mean aerodynamic chord.

C_L	lift coefficient, $\frac{-Z}{qS}$
C_X	longitudinal-force coefficient, $\frac{X}{qS}$
C_m	pitching-moment coefficient, $\frac{M'}{qS\bar{c}}$
C_l	rolling-moment coefficient, $\frac{L'}{qSb}$
C_n	yawing-moment coefficient, $\frac{N'}{qSb}$

~~CONFIDENTIAL~~

C_Y	lateral-force coefficient, $\frac{Y}{qS}$
X	force along X-axis
Y	force along Y-axis
Z	force along Z-axis
L'	moment about X-axis
M'	moment about Y-axis
N'	moment about Z-axis
q	free-stream dynamic pressure
R	Reynolds number based on \bar{c}
S	total wing area
b	wing span
\bar{c}	wing mean aerodynamic chord
M	Mach number
n_p	neutral-point location, percent \bar{c}
α	angle of attack of fuselage center line, deg
β	angle of sideslip, deg
δ_c	canard deflection with respect to fuselage center line, deg
δ_r	rudder deflection in streamline direction, deg
i_t	stabilizer incidence angle with respect to fuselage center line, deg
L/D	lift-drag ratio, $C_L/-C_X$
ΔC_X	incremental longitudinal-force coefficient above minimum

MODEL AND APPARATUS

A three-view drawing of the basic model is shown in figure 2 and details of the canard are shown in figure 3. The geometric characteristics of the model are presented in table I. A photograph of the configuration is shown in figure 4.

The model had a wing swept back 40° at the quarter-chord line, an aspect ratio of 4, a taper ratio of 0.5, and 10-percent-thick circular-arc sections normal to the quarter-chord line. Flat-sided 20-percent-chord ailerons having a trailing-edge thickness 0.5 of the hinge-line thickness were installed on the outboard 50 percent of the wing semispans.

The canard employed was of trapezoidal plan form and had a double-wedge section.

Force and moment measurements were made through the use of a six-component internal strain-gage balance.

TESTS AND CORRECTIONS

Test Conditions

The conditions for the tests were:

Mach number	1.89
Reynolds number, based on \bar{c}	0.28×10^6
Stagnation pressure, lb/sq in. abs	2
Stagnation temperature, $^\circ F$	100

Corrections and Accuracy

The tests were made in the $M = 2$ nozzle which, for pressures above 4 lb/sq in. abs produces a Mach number of 2.01. However, based upon a recent nozzle calibration for a stagnation pressure of 2 lb/sq in. abs, it was determined that the test section Mach number was 1.89 ± 0.02 . The base pressure was measured and the chord force was adjusted by equating the base pressure to the free-stream static pressure. The angles of attack and sideslip were corrected for the deflection of the balance and sting under load.

The estimated probable errors in the individual measured quantities are as follows:

C_L	±0.005
C_X	±0.002
C_m	±0.002
C_Y	±0.003
C_n	±0.0002
C_l	±0.0002
α , deg	±0.1
β , deg	±0.1
i_t , deg	±0.1
δ_c , deg	±0.1

RESULTS AND DISCUSSION

Pitching-Moment Characteristics

The canard control was designed to reduce the stability of the complete model at $M \approx 2$ so that about the same static margin would be obtained as that obtained at subsonic speeds. The desired changes in stability were estimated from the correlated results presented in reference 2.

The addition of the canard to the wing-body combination (fig. 5) greatly reduced the variation of C_m with α and the stability for the complete model with both the canard and horizontal tail on was about the same as that obtained for the configuration at subsonic speeds without the canard (ref. 2).

A trim angle of attack of about 6° (corresponding to a lift coefficient of about 0.26) was obtained with $i_t = -8^\circ$ (maximum obtainable) for the model without the canard surface. Installation of the canard resulted in an appreciable increase in maximum trim angle of attack. For zero deflection of the canard a maximum trim angle of attack of about 12.5° ($C_L \approx 0.53$) was obtained and by deflecting the canard to 30° the maximum trim angle of attack was increased to about 22° ($C_L \approx 0.84$). The installation of the canard surface introduced some nonlinearity in the variation of C_m with α , and the variation of C_m with δ_c was decreased considerably with increasing α .

Lift and Longitudinal-Force Characteristics

The variation of C_L and C_x with α for various configurations is presented in figures 6 and 7, respectively. Installation of the canard surface at $\delta_c = 0^\circ$ resulted in only a very slight increase in the lift-curve slope and a moderate increase in the minimum longitudinal-force coefficient. For $\delta_c = 30^\circ$ the longitudinal-force coefficient, of course, is considerably increased.

The variation of longitudinal force with lift (fig. 8) is slightly greater at low lifts for the model with the canard surface but at higher lifts becomes less than that for the model without the canard.

The maximum lift-drag ratio decreases as a result of installing the canard surface. (See fig. 9.) At the higher trim lift coefficients, however, which are made possible through the use of the canard, there is little difference in the values of L/D either with or without the canard.

Longitudinal Stability and Control

The variation of C_m , C_x , and α with C_L for various canard deflections at a constant i_t of -8° is shown in figure 10. The maximum trim lift coefficient obtained with $\delta_c = 30^\circ$ is about 0.84. A nonlinear variation of C_m with C_L is indicated such that during maneuvering flight it would be difficult to perform constant radius turns.

A relatively large increase in stability occurs with increasing lift coefficient (figs. 10 and 11). The neutral-point location at $\delta_c = 0^\circ$ ($C_L \approx 0.52$) is about 0.363 which is about the same as at subsonic speeds for the basic model with no canard surface (see ref. 2) but this value increases to about 0.643 for $\delta_c = 30^\circ$ ($C_L \approx 0.84$). The variation of δ_c with C_L becomes increasingly nonlinear with increasing C_L to the extent that it is clearly evident that canard deflections beyond 20° at the most are inutile (see fig. 11).

The lift-drag ratio, which is quite low even at zero canard deflection, reduces to slightly less than 2 at the maximum lift coefficient obtained (fig. 11).

Lateral Stability Characteristics

The aerodynamic characteristics in sideslip at $\alpha = 0^\circ$ and $\delta_c = 0^\circ$ (fig. 12) indicate a positive dihedral effect ($-C_{l\beta}$) and positive

directional stability ($C_{n\beta}$). A restoring moment in yaw is indicated for the complete model throughout a sideslip range to about 44° . The presence of the canard at zero deflection appears to have little effect on the lateral stability characteristics. It might be expected, however, that at higher angles of attack and for canard deflections other than zero the characteristics in sideslip could be altered considerably.

CONCLUSIONS

The results of an investigation at a Mach number of 1.89 and a simulated pressure altitude of about 88,000 feet of a model of a supersonic aircraft configuration equipped with a canard control surface in addition to a conventional horizontal stabilizer indicated the following conclusions:

1. The maximum trim lift coefficient was increased from about 0.26 for the model with the canard off to about 0.84 with the canard on.
2. The ratio of lift to drag at the maximum trim lift coefficient was slightly less than 2.
3. The neutral-point location for a zero canard deflection was at about 36 percent of the mean aerodynamic chord but moved rearward to about 64 percent for a canard deflection of 30° .
4. The presence of the canard at zero deflection and zero angle of attack had little effect on the lateral characteristics.

Langley Aeronautical Laboratory,
National Advisory Committee for Aeronautics,
Langley Field, Va., August 4, 1954.

REFERENCES

1. Spearman, M. Leroy, and Palazzo, Edward B.: An Investigation of a Supersonic Aircraft Configuration Having a Tapered Wing With Circular-Arc Sections and 40° Sweepback - Static Longitudinal and Lateral Stability and Control Characteristics at a Mach Number of 1.89. NACA RM L54G26a, 1954.
2. Spearman, M. Leroy, and Robinson, Ross B.: The Aerodynamic Characteristics of a Supersonic Aircraft Configuration With a 40° Swept-back Wing Through a Mach Number Range From 0 to 2.4 As Obtained From Various Sources. NACA RM L52A21, 1952.

TABLE I.- GEOMETRIC CHARACTERISTICS OF MODEL

Wing:

Area, sq ft	1.158
Span, ft	2.155
Aspect ratio	4
Sweepback of quarter-chord line, deg	40
Taper ratio	0.5
Mean aerodynamic chord	0.557
Airfoil section normal to quarter-chord line	10-percent-thick, circular-arc
Twist, deg	0

Canard:

Area, sq ft	0.094
Aspect ratio	2.67
Sweepback of leading edge, deg	14
Taper ratio	0.5
Airfoil section	10-percent-thick, diamond

Horizontal tail:

Area, sq ft	0.196
Aspect ratio	3.72
Sweepback of quarter-chord line, deg	40
Taper ratio	0.5
Airfoil section	NACA 65-008

Vertical tail:

Area (exposed), sq ft	0.172
Aspect ratio (based on exposed area and span)	1.17
Sweepback of leading edge, deg	40.6
Taper ratio	0.337
Airfoil section, root	NACA 27-010
Airfoil section, tip	NACA 27-008

Fuselage:

Fineness ratio (neglecting canopies)	9.4
--	-----

Miscellaneous:

Tail length from $\bar{c}/4$ wing to $\bar{c}_t/4$ tail, ft	0.917
Tail height, wing semispans above fuselage center line	0.153

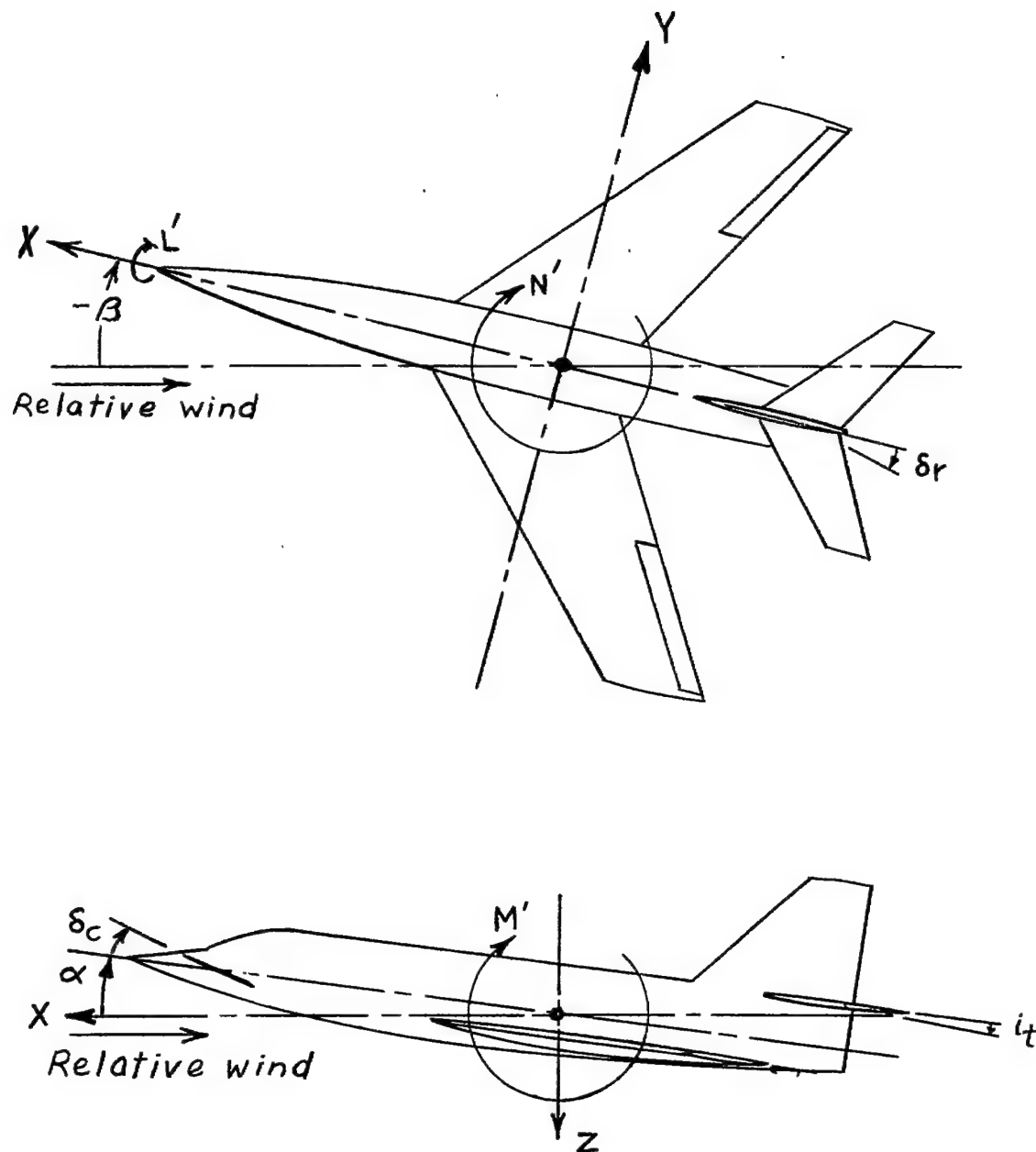


Figure 1.- System of stability axes. Arrows indicate positive values.

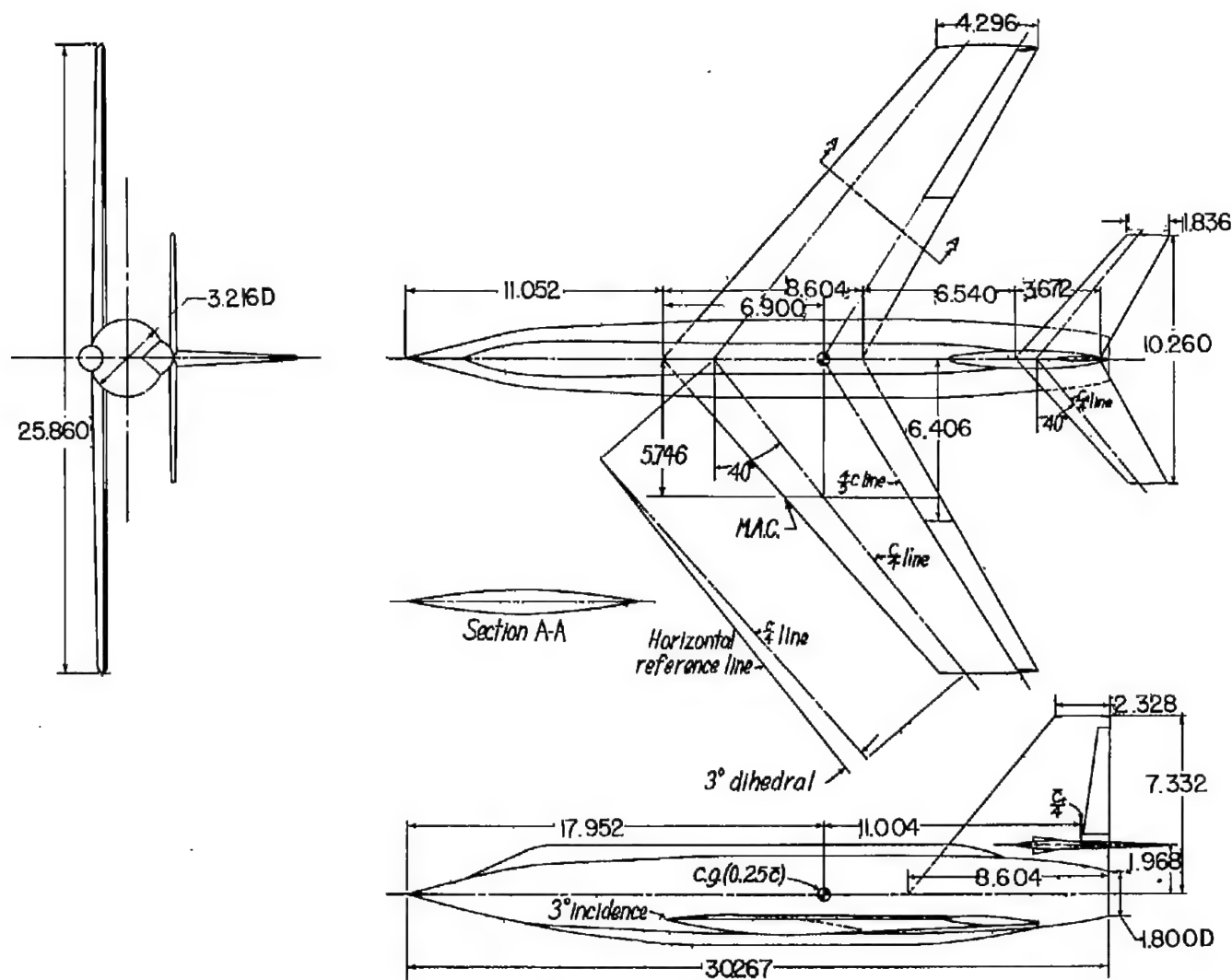


Figure 2.- Details of model of supersonic aircraft configuration. Dimensions are in inches unless otherwise noted.

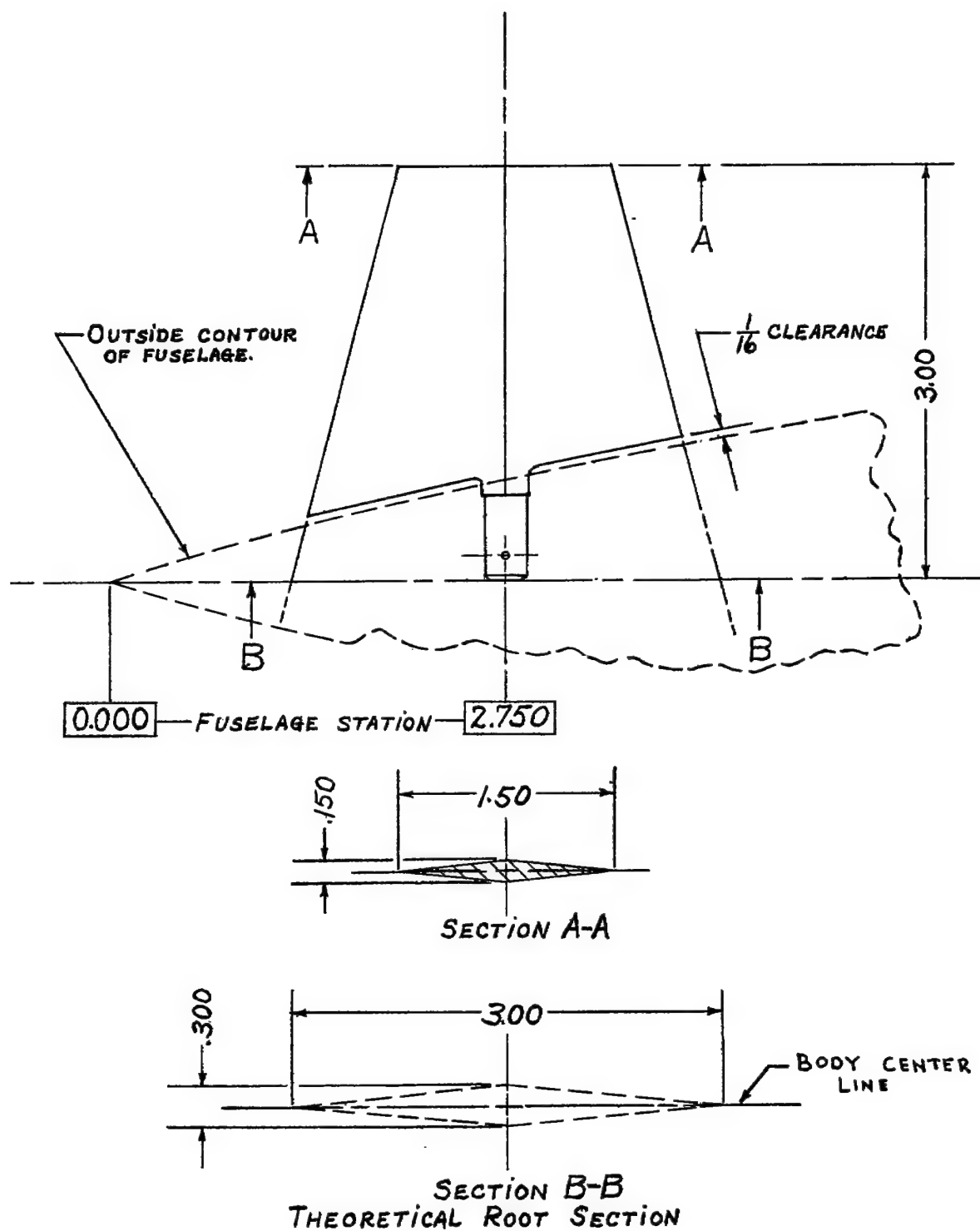


Figure 3.- Dimensions of canard. All dimensions are in inches.

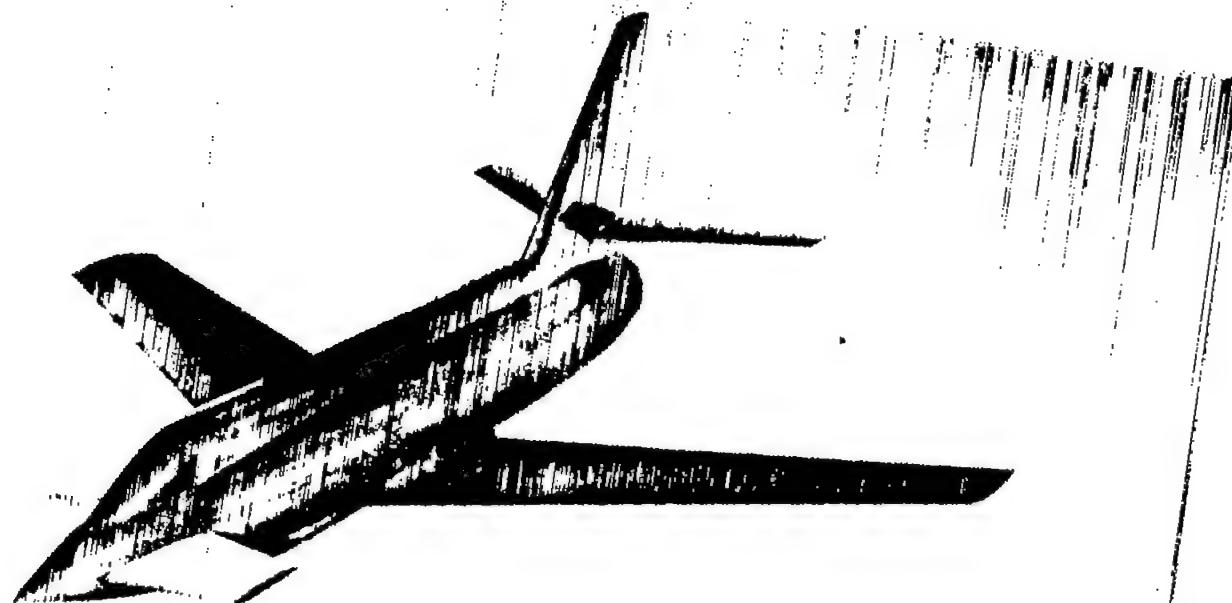


Figure 4.- Photograph of model.

L-64078.2

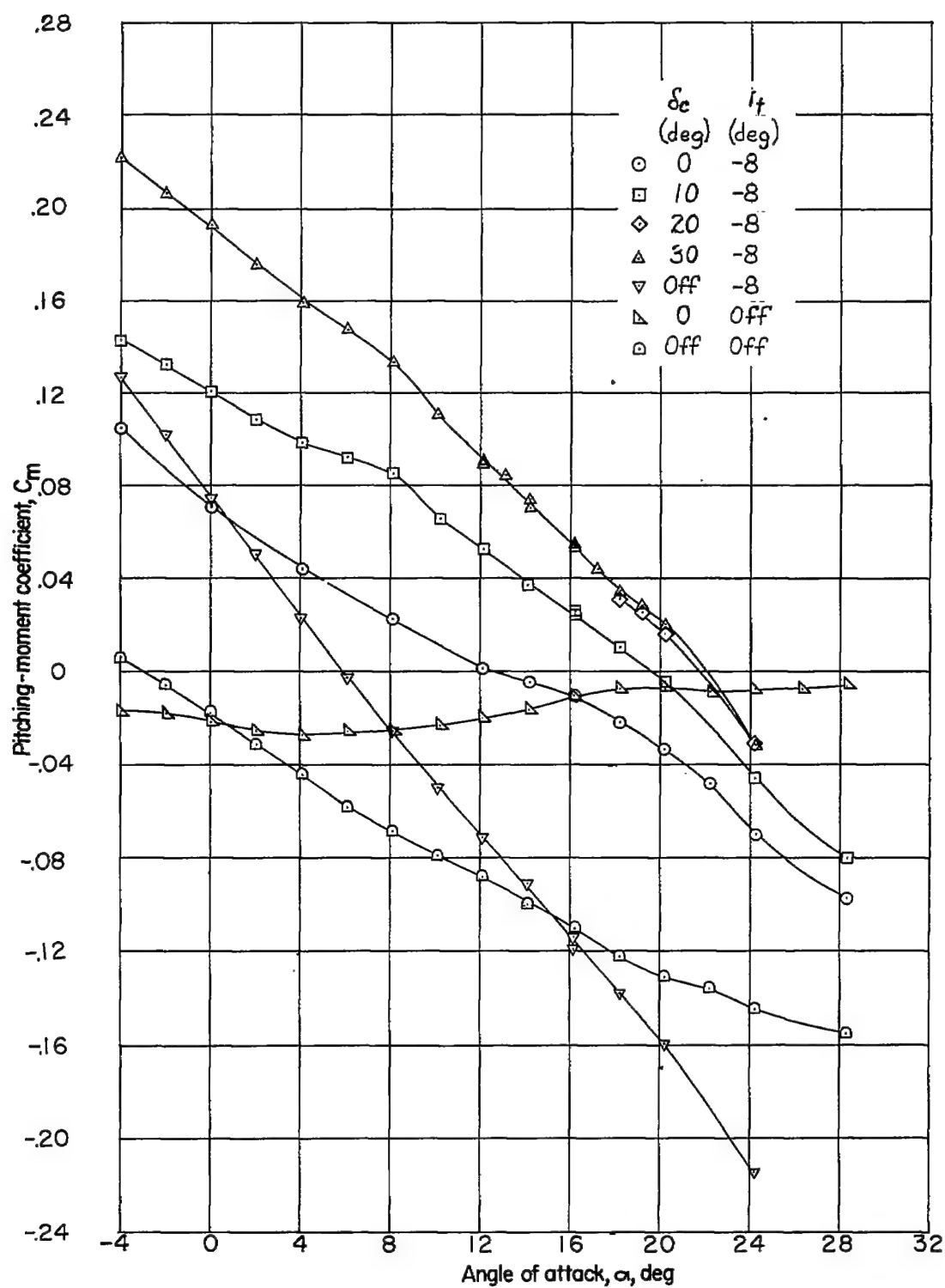
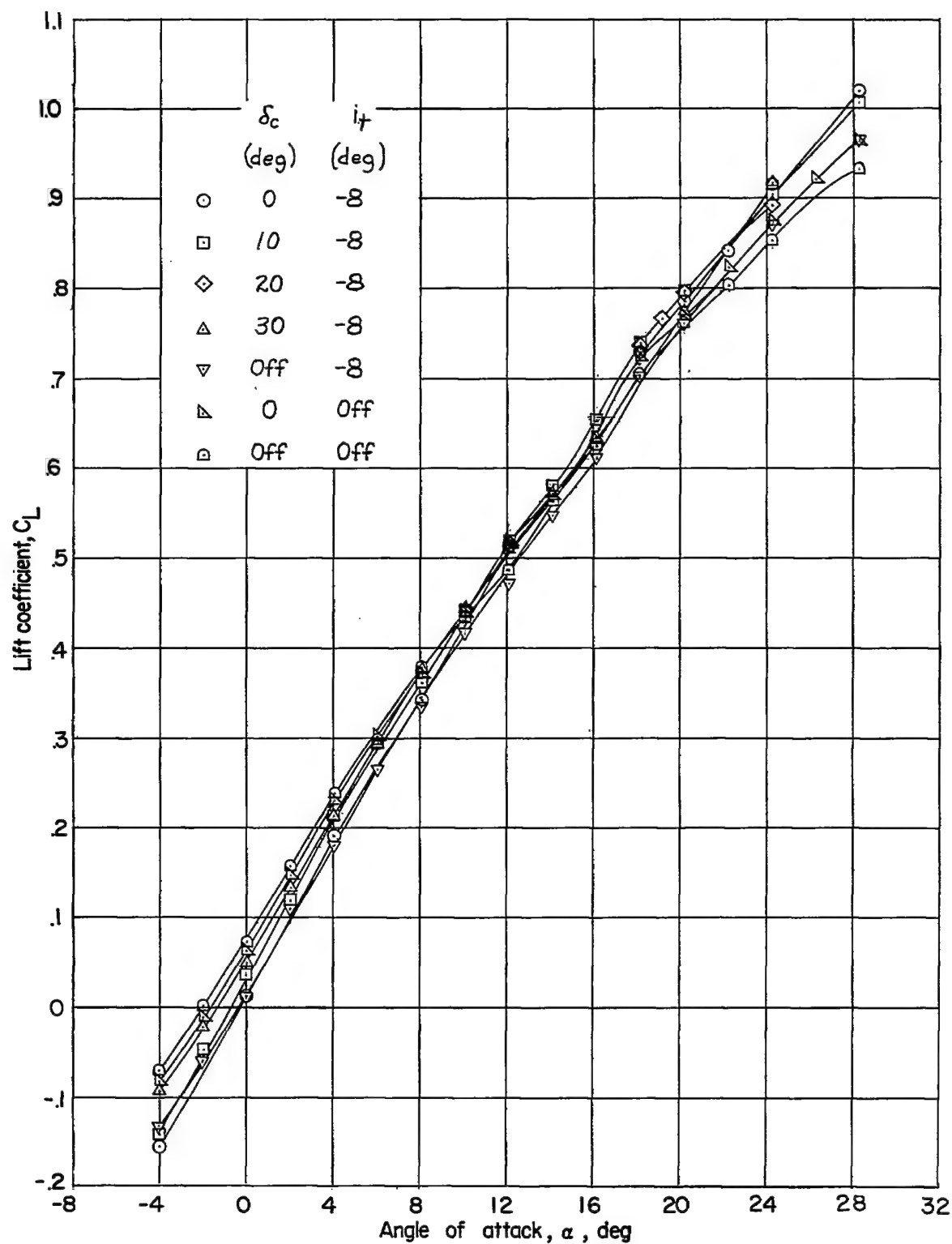


Figure 5.- Variation of pitching-moment coefficient with angle of attack.
 $M = 1.89$.

Figure 6.- Variation of lift coefficient with angle of attack. $M = 1.89$.

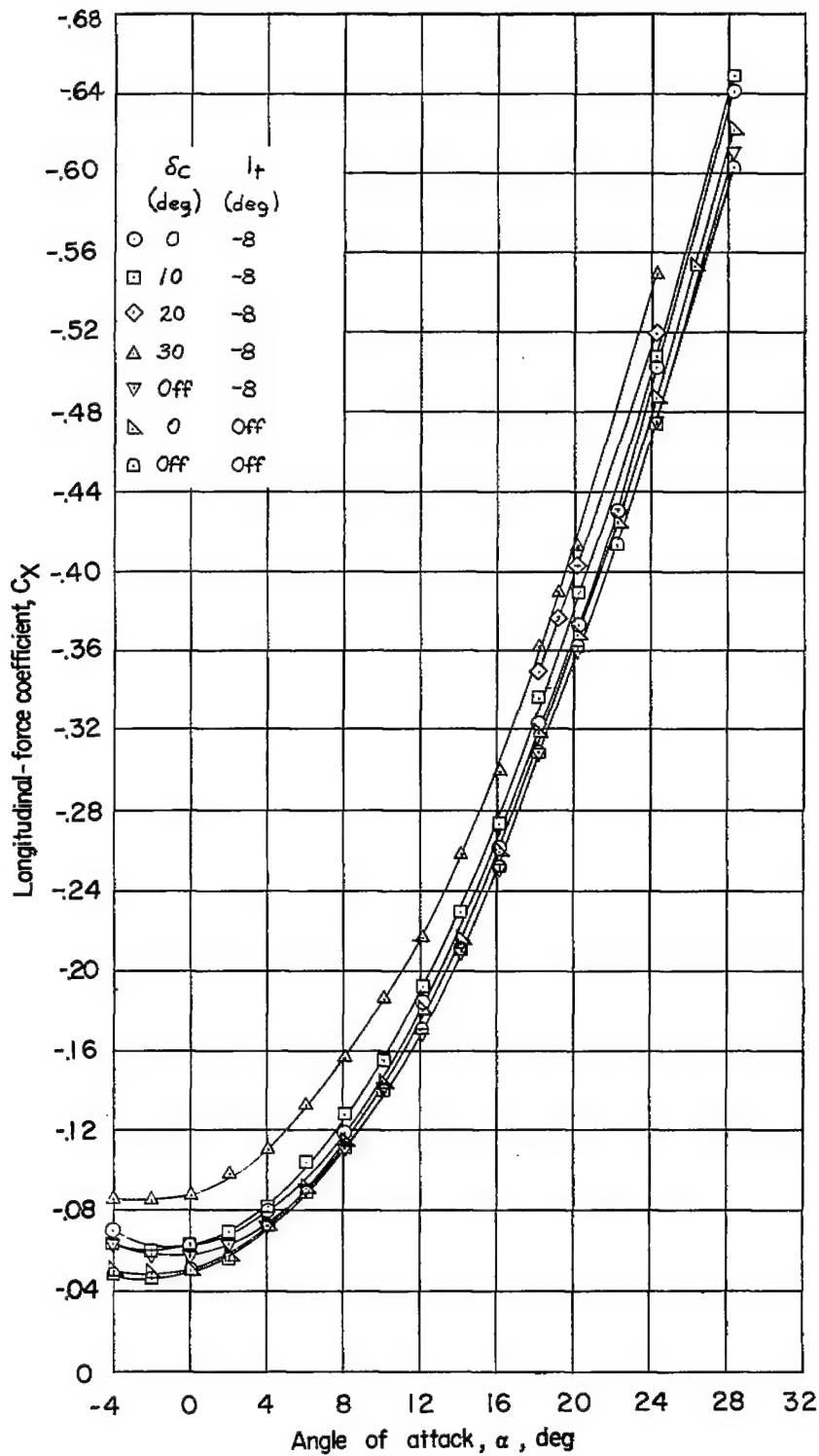


Figure 7.- Variation of longitudinal-force coefficient with angle of attack. $M = 1.89$.

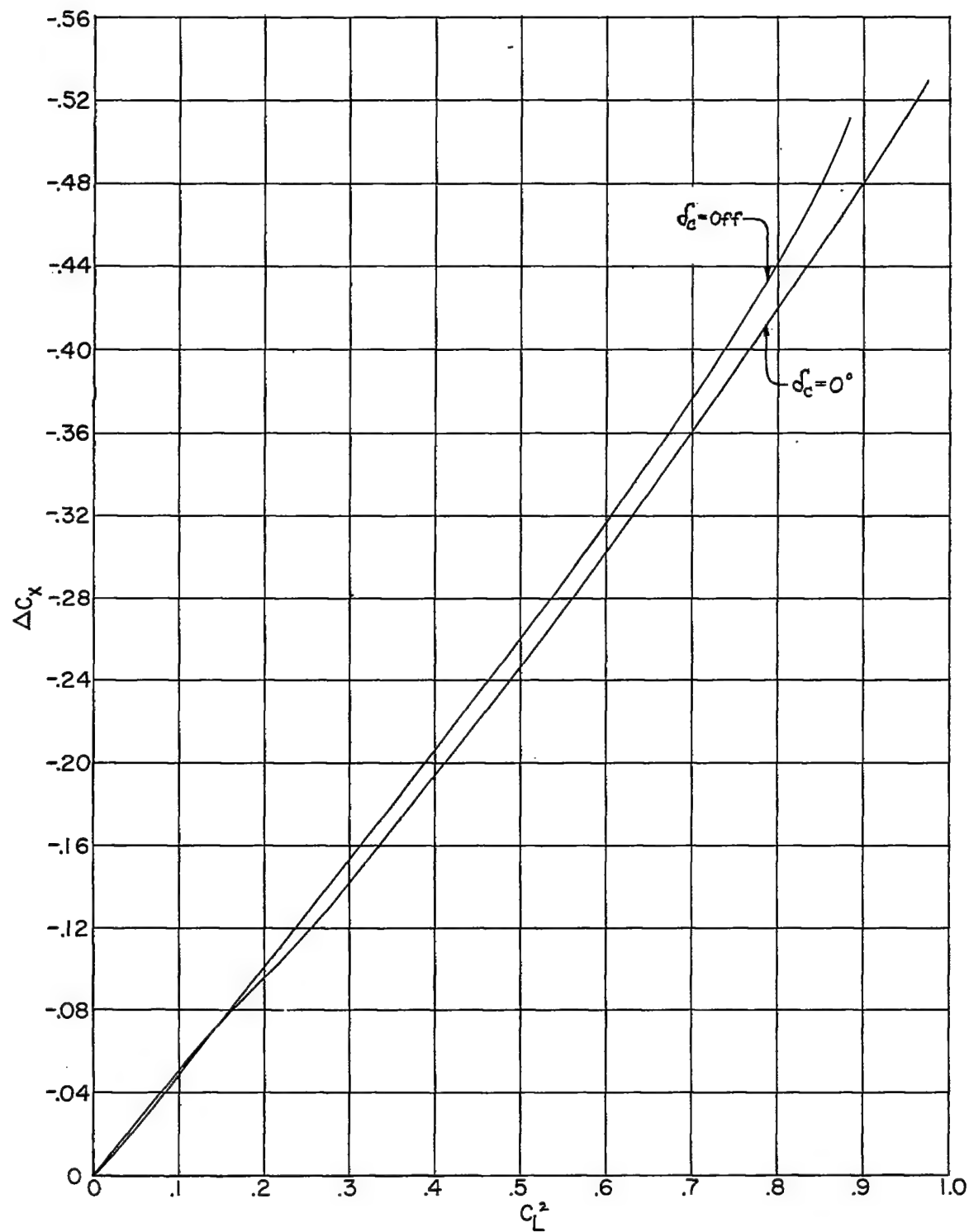


Figure 8.- Variation of longitudinal force with lift. $M = 1.89$; $i_t = -8^\circ$.

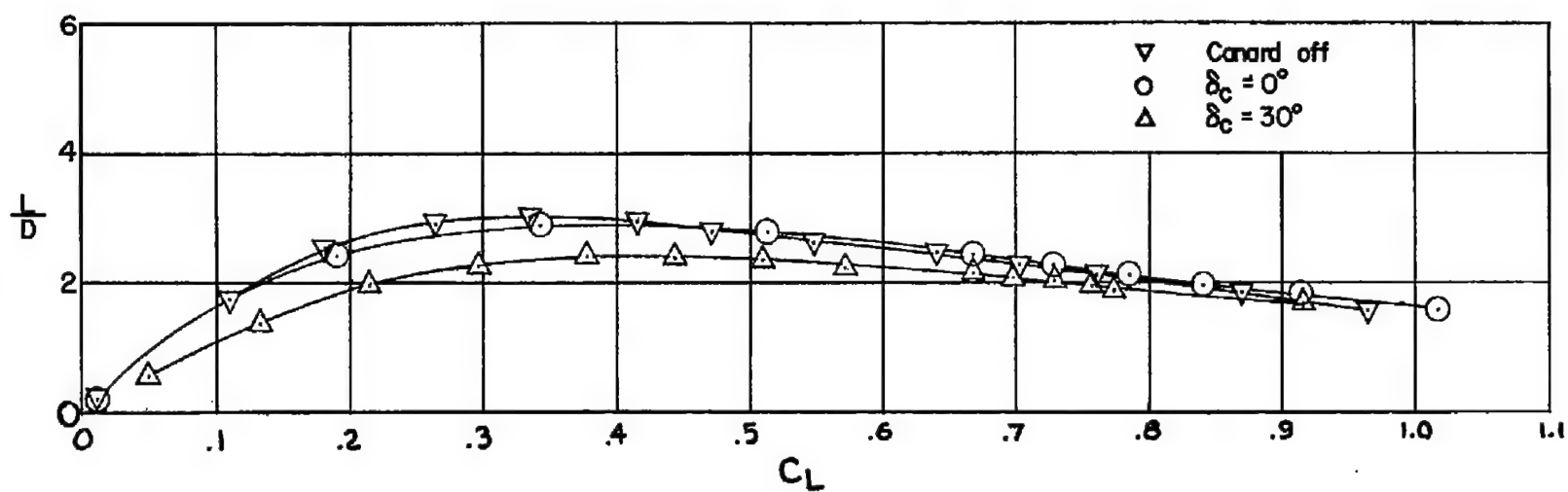


Figure 9.- Variation of lift-drag ratio with lift coefficient. $M = 1.89$;
 $i_t = -8^\circ$.

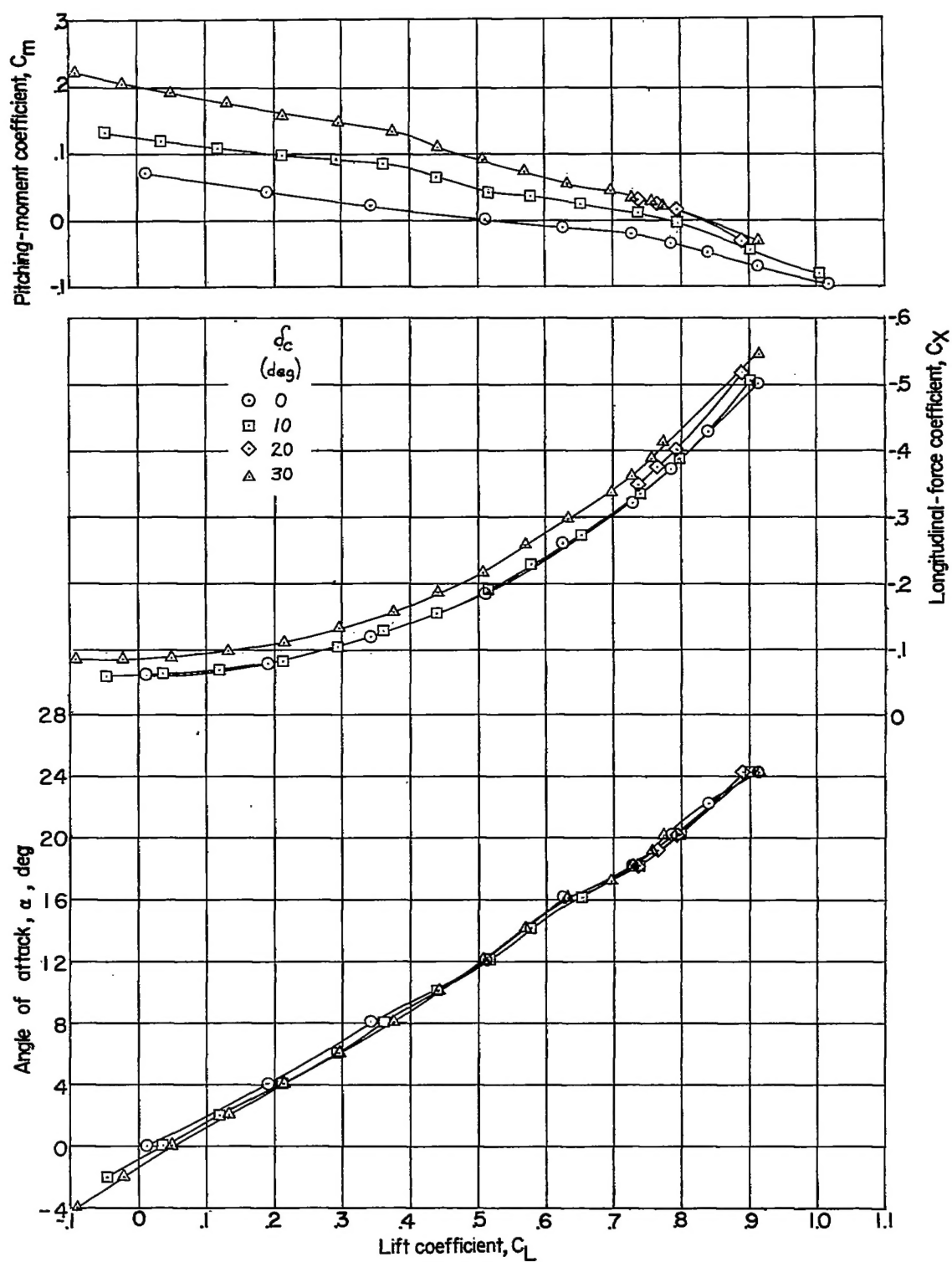


Figure 10.- Aerodynamic characteristics in pitch. $M = 1.89$; $i_t = -8^\circ$.

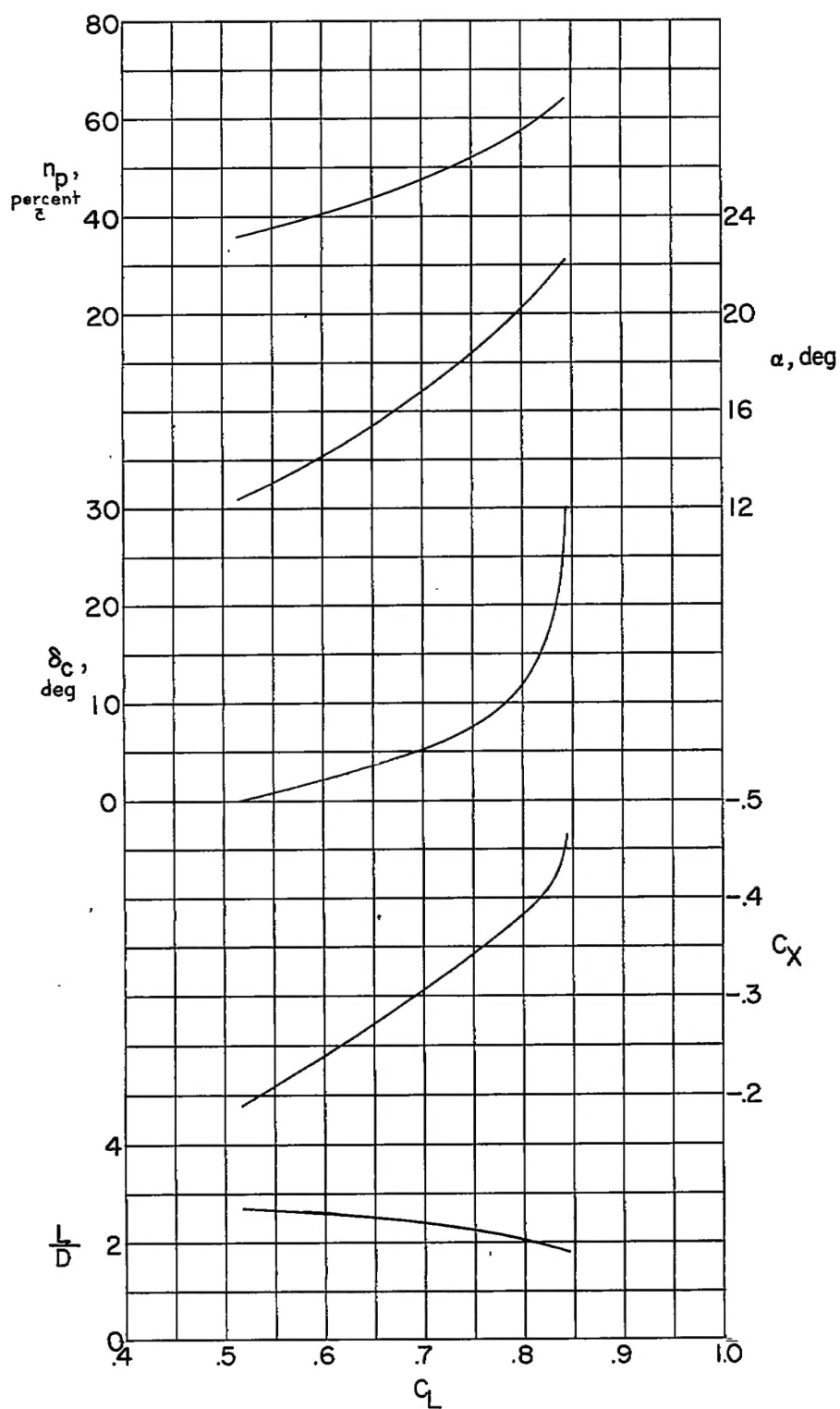


Figure 11.- Trim longitudinal characteristics. $M = 1.89$; $i_t = -8^\circ$.

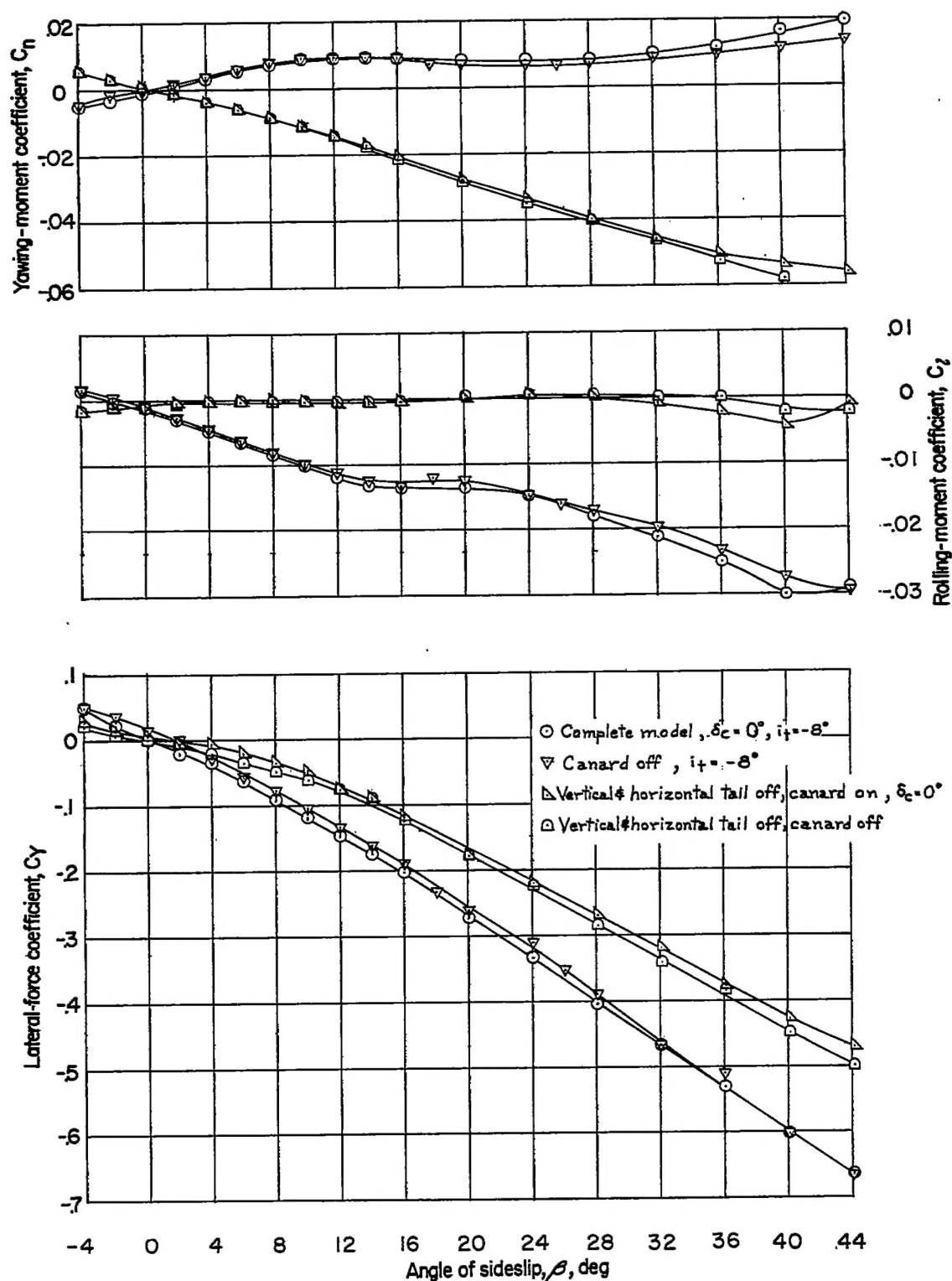


Figure 12.- Aerodynamic characteristics in sideslip for various configurations. $M = 1.89$; $\alpha = 0^\circ$.

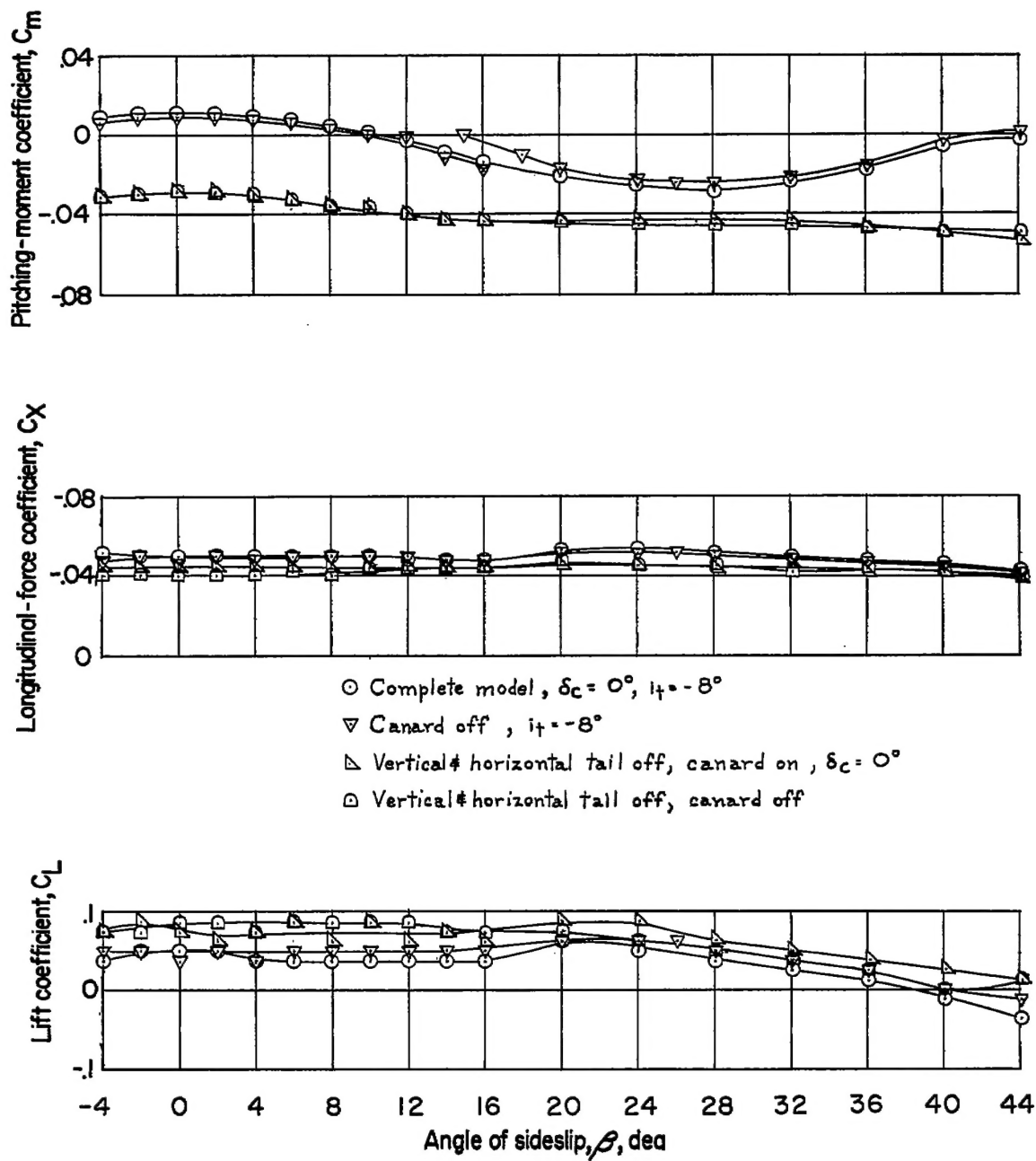


Figure 12.- Concluded.